

# Instance-Level Salient Object Segmentation

(Supplemental Materials)

Guanbin Li<sup>1,2</sup>    Yuan Xie<sup>1</sup>    Liang Lin<sup>1</sup>    Yizhou Yu<sup>2\*</sup>

<sup>1</sup>Sun Yat-sen University

<sup>2</sup>The University of Hong Kong

## 1. Comparison of Precision-recall Curves on MSRA-B, ECSSD and SOD Datasets

We compare the proposed MSRNet with 8 other state-of-the-art salient region detection methods, including GC [2], DRFI [3], LEGS [7], MC [9], MDF [4], DCL<sup>+</sup> [5], DHSNet [6] and RFCN [8]. The last six are the latest deep learning based methods. We use the original implementations provided by the authors in this comparison. A comparison of PR curves on MSRA-B, ECSSD and SOD datasets is shown in Fig. 1. As shown in Fig. 1, our proposed MSRNet consistently has the highest PR curve on MSRA-B, ECSSD and SOD datasets.

## 2. Comparison of Average Precision, Recall and F-measure

We also report performance comparisons in average precision, recall and F-measure using an adaptive threshold among 9 salient region detection methods on 6 datasets. The adaptive threshold is set to twice the mean saliency value of each saliency map as suggested in [1]. As shown in Fig. 2, our proposed MSRNet achieves the best performance in average F-measure on all datasets.

## 3. Visual Comparison of Saliency Maps from State-of-the-art Methods

Figs. 3 and 4 show more visual comparisons of salient region detection results generated from 9 different models, including our MSRNet. The ground truth (GT) is shown in the last column. MSRNet consistently produces saliency maps closest to the ground truth. We compare MSRNet against GC [2], DRFI [3], LEGS [7], MC [9], MDF [4], DCL<sup>+</sup> [5], DHSNet [6] and RFCN [8].

## 4. Examples of Salient Instance Segmentation Results

Figs. 5 and 6 show more examples of salient instance segmentation results from our MSRNet based framework. Our proposed MSRNet can generate very promising results for salient region detection as well as salient contour detection. For salient instance segmentation, as shown in the figures, the proposed MSRNet based framework can handle challenging cases where multiple salient object instances are spatially connected to each other.

## References

- [1] R. Achanta, S. Hemami, F. Estrada, and S. Susstrunk. Frequency-tuned salient region detection. In *CVPR*, 2009. 1
- [2] M.-M. Cheng, N. J. Mitra, X. Huang, P. H. Torr, and S.-M. Hu. Global contrast based salient region detection. *TPAMI*, 37(3):569–582, 2015. 1
- [3] H. Jiang, J. Wang, Z. Yuan, Y. Wu, N. Zheng, and S. Li. Salient object detection: A discriminative regional feature integration approach. In *CVPR*, 2013. 1
- [4] G. Li and Y. Yu. Visual saliency based on multiscale deep features. In *CVPR*, 2015. 1
- [5] G. Li and Y. Yu. Deep contrast learning for salient object detection. In *CVPR*, 2016. 1
- [6] N. Liu and J. Han. Dhsnet: Deep hierarchical saliency network for salient object detection. In *CVPR*, 2016. 1, 2

---

\*Corresponding author (email: yizhouy@acm.org).

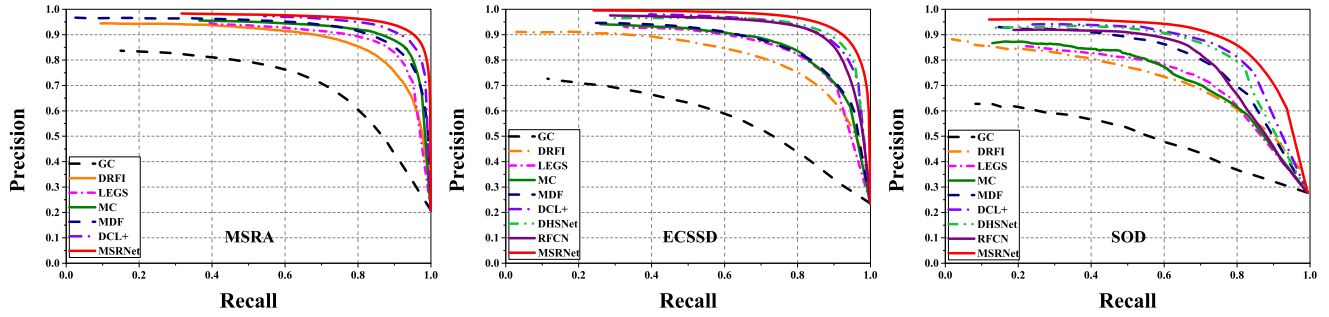


Figure 1. Comparison of precision-recall curves among 9 salient region detection methods on 3 datasets. Our MSRNet consistently outperforms other methods across all the three testing datasets. Note that RFCN [8] and DHSNet [6] include the testing set of MSRA-B in their training data, therefore RFCN and DHSNet are not included in the comparison on this dataset.

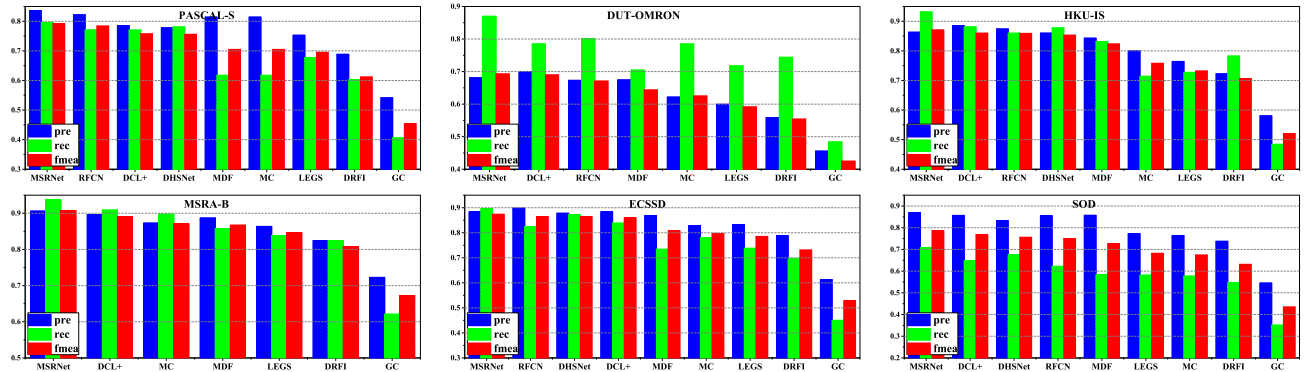


Figure 2. Comparison of average precision, recall and F-measure (computed using a per-image adaptive threshold) among 9 different methods on 6 datasets. Note that RFCN [8] and DHSNet [6] include the testing set of MSRA-B in their training data, therefore RFCN and DHSNet are not included in the comparison on this dataset. DHSNet [6] also includes the testing set of DUT-OMRON in its training data, therefore DHSNet is not included in the comparison on the DUT-OMRON dataset either.

[7] L. Wang, H. Lu, X. Ruan, and M.-H. Yang. Deep networks for saliency detection via local estimation and global search. In *CVPR*, 2015. 1

[8] L. Wang, L. Wang, H. Lu, P. Zhang, and X. Ruan. Saliency detection with recurrent fully convolutional networks. In *ECCV*, 2016. 1, 2

[9] R. Zhao, W. Ouyang, H. Li, and X. Wang. Saliency detection by multi-context deep learning. In *CVPR*, 2015. 1

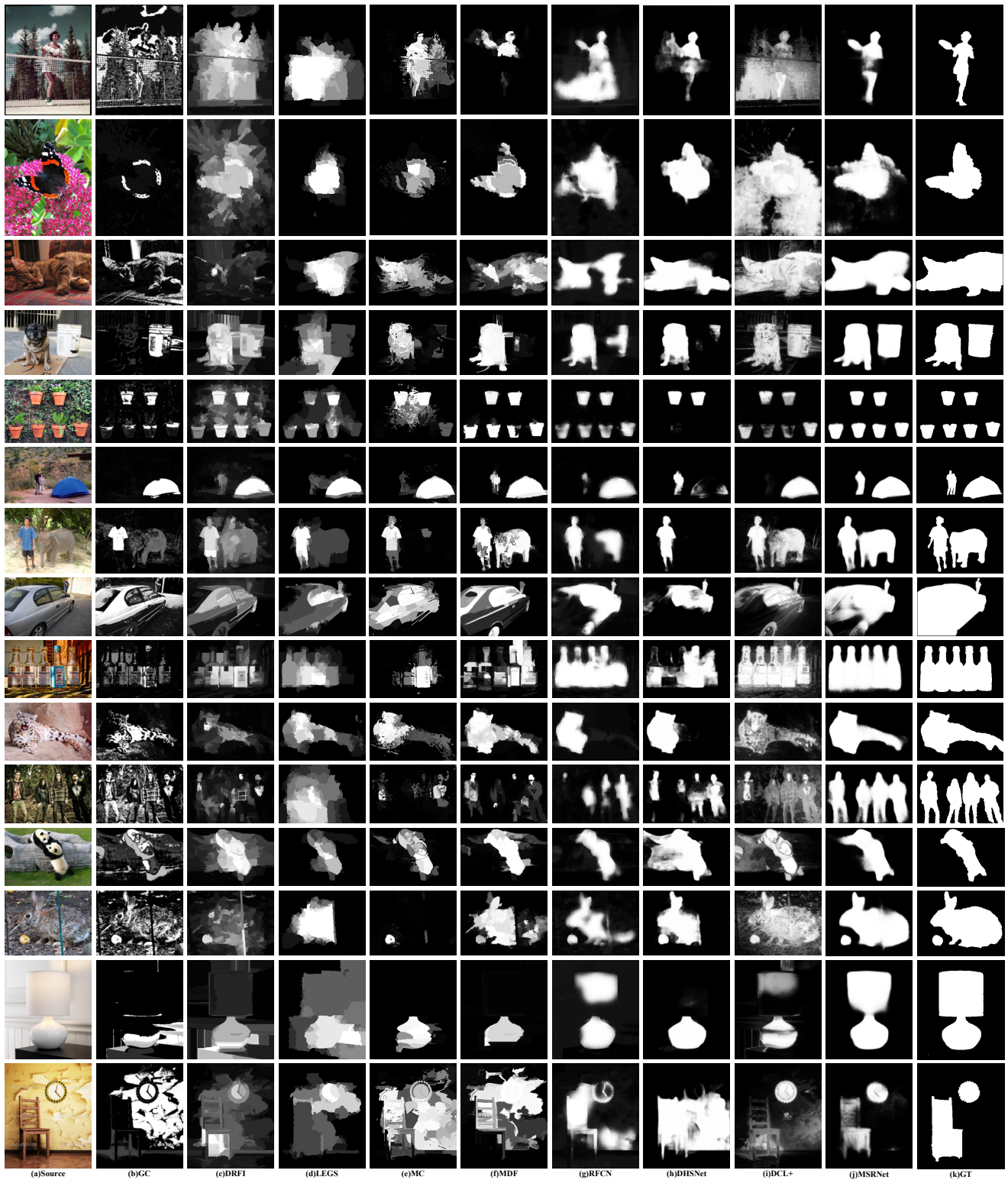


Figure 3. Visual comparison of saliency maps from state-of-the-art methods, including our MSRNet. The ground truth (GT) is shown in the last column. MSRNet consistently produces saliency maps closest to the ground truth.

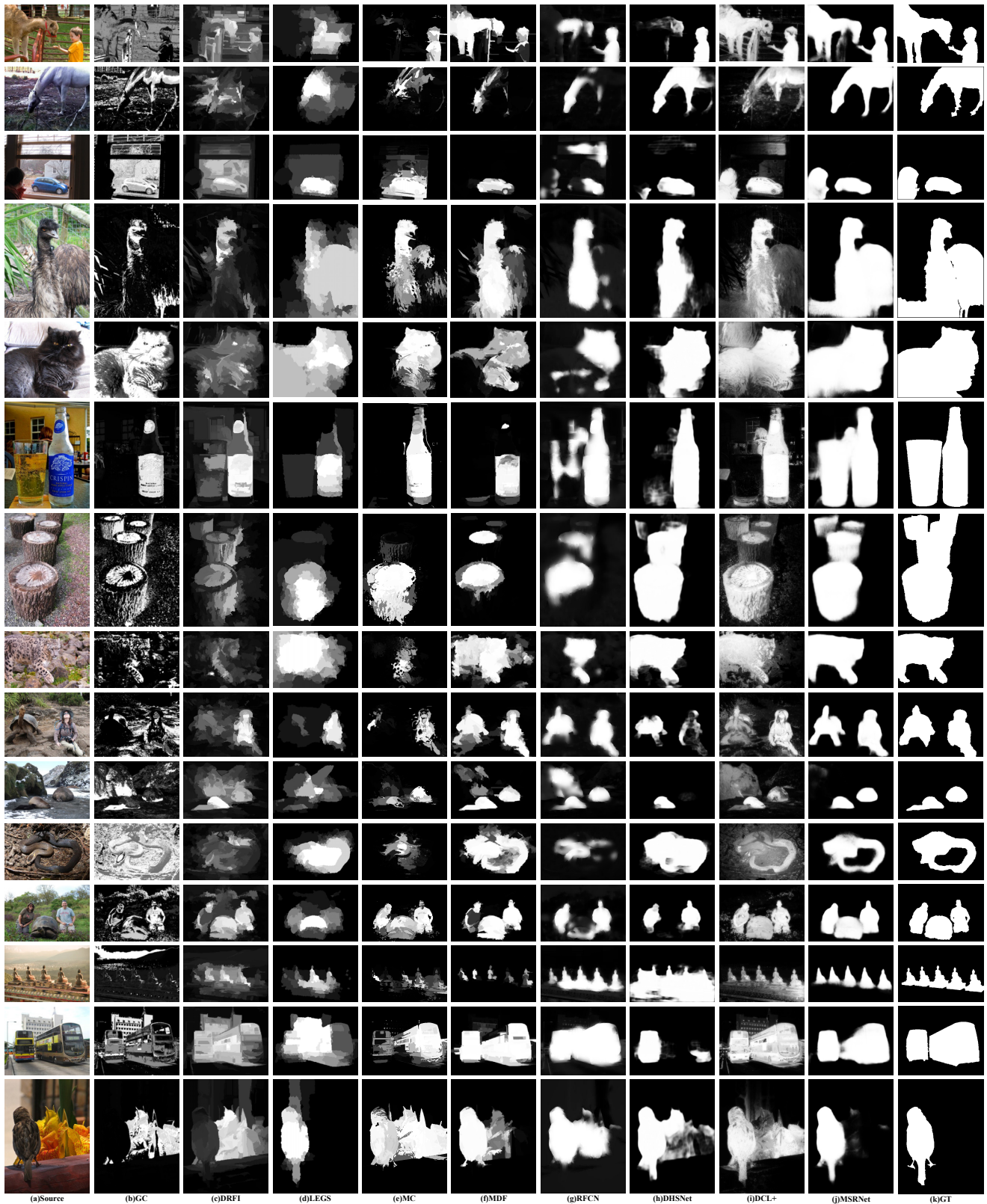


Figure 4. Visual comparison of saliency maps from state-of-the-art methods, including our MSNet. The ground truth (GT) is shown in the last column. MSNet consistently produces saliency maps closest to the ground truth.

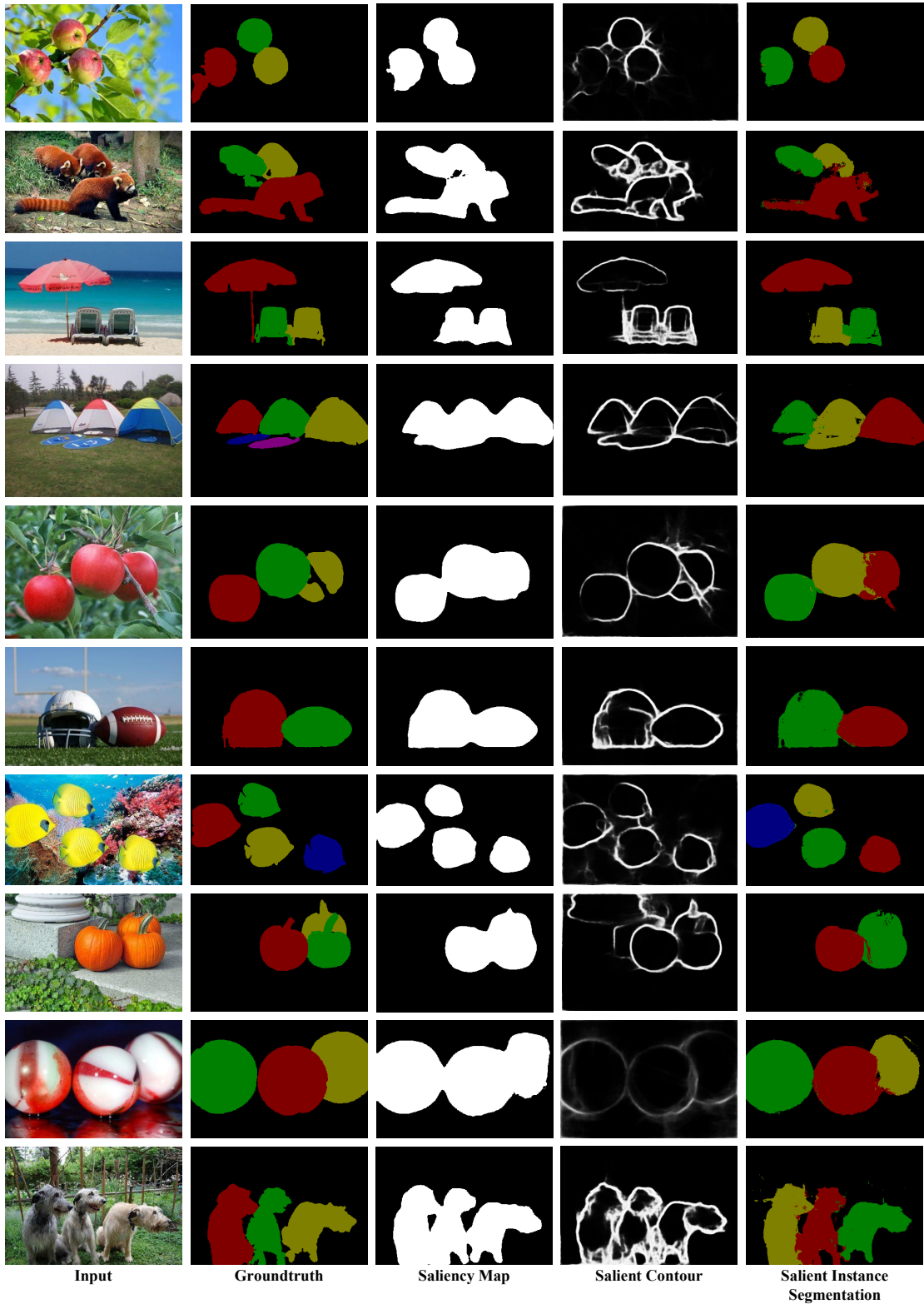


Figure 5. Examples of salient instance segmentation results from our MSRNet based framework. From left to right, we show the input image, the ground truth of salient instance segmentation, the binarized saliency map generated from MSRNet, salient object contour from MSRNet, and our salient instance segmentation result. In the salient instance segmentation results, different colors indicate different object instances in detected salient regions.



Figure 6. Examples of salient instance segmentation results from our MSRNet based framework. From left to right, we show the input image, the ground truth of salient instance segmentation, the binarized saliency map generated from MSRNet, salient object contour from MSRNet, and our salient instance segmentation result. In the salient instance segmentation results, different colors indicate different object instances in detected salient regions.